Bis-Adducts of Substituted Phenylethynyl on a $Ru_2(DMBA)_4$ Core: Effect of Donor/Acceptor Modifications

Stephanie K. Hurst, Guo-Lin Xu, and Tong Ren*

Department of Chemistry, University of Miami, Coral Gables, Florida 33124

Received May 29, 2003

The reactions between arylethynes (either BuLi activated or Et_3N assisted) and $Ru_2(RDMBA)_4X_2$, where R*DMBA* is either *N*,*N*′-dimethylbenzamidinate (R = H) or *N*,*N*′-dimethyl-*m*-methoxybenzamidinate (R = *m*-MeO) and X is either Cl^- or NO_3^-, resulted in the compounds $Ru_2(RDMBA)_4(C{\equiv}CC_6H_4Y)_2$ (Y = H (**1a**,**b**), 4-NO_2 (**2a**,**b**), 4-CN (**3a**,**b**), 3-CN (**4a**,**b**), 4-NMe_2 (**5a**,**b**); R = H (**a**), *m*-MeO (**b**)). The single-crystal X-ray diffraction study of **1b** and **2a** revealed the linear alignment of the arylethynyl ligands along the Ru−Ru vector. All of the compounds display two Ru-based one-electron processes, an oxidation and a reduction, and their electrode potentials correlate linearly with the Hammett constants of substituent Y. Compounds **5a**,**b** display an additional pair of one-electron processes attributed to the oxidation of 4-NMe_2 groups, on the basis of which an extensive electron delocalization along the metallayne backbone was inferred.

Introduction

Dinuclear paddlewheel species continue to attract significant attention, due to the diversity in both metal centers and bridging ligands, as well as their interesting electrochemical, magnetic, and other properties.[1,2] Facile electron delocalizations between dinuclear units linked via a π-delocalized framework have been demonstrated by the laboratories of Cotton,[3] Bursten and Chisholm,[4,5] and Ren,[6,7] revealing the possibility of realizing molecular electronic wires based on these paddlewheel species.[8,9] To achieve this goal, the ability to precisely control the electronic properties of paddlewheel species is crucial. Previously, substituent effects in paddlewheel species were explored in our laboratory on a series of $M_2(DArF)_4$ compounds with M = Mo, Ni, Ru, Rh and *D*Ar*F* = diarylformamidinate.[10−16] Initial studies of Mo_2 and Ni_2 series revealed that there is a linear correlation between electrode potentials of metal-based redox processes and the Hammett constants (σ) of the phenyl substituent on *D*Ar*F* ligands, and both the optical and structural features were unaltered by the substituents.[10−12] Similar results were found for the series of $Rh_2(DArF)_4$ compounds and $Ru_2(DArF)_4$ compounds bearing either chloro or phenylethynyl axial ligands in our laboratory,[13−16] $Re_2(DArF)_4Cl_2$ and $Cr_2(DArF)_4$ compounds in the laboratory of Eglin,[17,18] and $Ru_2(X\text{-ap})_4Cl$ compounds (X-ap = substituted 2-anilinopyridinates) in the laboratory of Bear and Kadish.[19] It was concluded that the phenyl substitution of the bridging ligands imparts an inductive effect on the dinuclear core.[20] The significance of substituent effects in the chemistry of transition-metal complexes of both alkynyl and other unsaturated carbon ligands such as allenylidene and cumulenylidene is also well documented.[21,22] For example, the presence of strong donor or acceptor groups has been a hallmark of mononuclear complexes with enhanced nonlinear optical properties.[23]

We reported recently the synthesis of $Ru_2(DMBA)_4Cl_2$ and its reactions with lithiated alkynyls to yield $Ru_2(DMBA)_4(C_2R)_2$ (R = H, $SiMe_3$, C_2SiMe_3, C_2H, Ph).[24] The

* To whom correspondence should be addressed. E-mail: tren@miami.edu. Tel: (305) 284-6617. Fax: (305) 284-1880.

(1) Cotton, F. A.; Walton, R. A. *Multiple Bonds between Metal Atoms*; Oxford University Press: Oxford, U.K., 1993.
(2) Cotton, F. A.; Lin, C.; Murillo, C. A. *Acc. Chem. Res.* **2001**, *34*, 759 and references therein.
(3) Cotton, F. A.; Donahue, J. P.; Murillo, C. A. *J. Am. Chem. Soc.* **2003**, *125*, 5436.
(4) Bursten, B. E.; Chisholm, M. H.; Clark, R. J. H.; Firth, S.; Hadad, C. M.; MacIntosh, A. M.; Wilson, P. J.; Woodward, P. M.; Zaleski, J. M. *J. Am. Chem. Soc.* **2002**, *124*, 3050.
(5) Bursten, B. E.; Chisholm, M. H.; Clark, R. J. H.; Firth, S.; Hadad, C. M.; Wilson, P. J.; Woodward, P. M.; Zaleski, J. M. *J. Am. Chem. Soc.* **2002**, *124*, 12244.
(6) Ren, T.; Zou, G.; Alvarez, J. C. *Chem. Commun.* **2000**, 1197.
(7) Xu, G.-L.; Zou, G.; Ni, Y.-H.; DeRosa, M. C.; Crutchley, R. J.; Ren, T. *J. Am. Chem. Soc.* **2003**, *125*, 10057.
(8) Paul, F.; Lapinte, C. *Coord. Chem. Rev.* **1998**, *178−180*, 431.
(9) Ren, T.; Xu, G.-L. *Comments Inorg. Chem.* **2002**, *23*, 355.
(10) Lin, C.; Protasiewicz, J. D.; Smith, E. T.; Ren, T. *J. Chem. Soc., Chem. Commun.* **1995**, 2257.
(11) Lin, C.; Protasiewicz, J. D.; Ren, T. *Inorg. Chem.* **1996**, *35*, 7455.
(12) Lin, C.; Protasiewicz, J. D.; Smith, E. T.; Ren, T. *Inorg. Chem.* **1996**, *35*, 6422.
(13) Lin, C.; Ren, T.; Valente, E. J.; Zubkowski, J. D.; Smith, E. T. *Chem. Lett.* **1997**, 753.
(14) Lin, C.; Ren, T.; Valente, E. J.; Zubkowski, J. D. *J. Chem. Soc., Dalton Trans.* **1998**, 571.
(15) Lin, C.; Ren, T.; Valente, E. J.; Zubkowski, J. D. *J. Organomet. Chem.* **1999**, *579*, 114.
(16) Ren, T.; Lin, C.; Valente, E. J.; Zubkowski, J. D. *Inorg. Chim. Acta* **2000**, *297*, 283.
(17) Carlson-Day, K. M.; Eglin, J. L.; Lin, C.; Smith, L. T.; Staples, R. J.; Wipf, D. O. *Polyhedron* **1999**, *18*, 817.
(18) Eglin, J. L.; Lin, C.; Ren, T.; Smith, L.; Staples, R. J.; Wipf, D. O. *Eur. J. Inorg. Chem.* **1999**, 2095.
(19) Kadish, K. M.; Wang, L.-L.; Thuriere, A.; Caemelbecke, E. V.; Bear, J. L. *Inorg. Chem.* **2003**, *42*, 834.
(20) Ren, T. *Coord. Chem. Rev.* **1998**, *175*, 43.
(21) Bruce, M. I. *Chem. Rev.* **1998**, *98*, 2797.
(22) Bruce, M. I. *Coord. Chem. Rev.* **1997**, *166*, 91.
(23) Whittall, I. R.; McDonagh, A. M.; Humphrey, M. G.; Samoc, M. *Adv. Organomet. Chem.* **1999**, *43*, 349.
(24) Xu, G. L.; Campana, C.; Ren, T. *Inorg. Chem.* **2002**, *41*, 3521.

10.1021/om030401y CCC: $25.00
Publication on Web 08/23/2003

Chart 1. Structure of Bis(phenylethynyl) Adducts on the $Ru_2(DMBA)_4$ Core and Their Designations

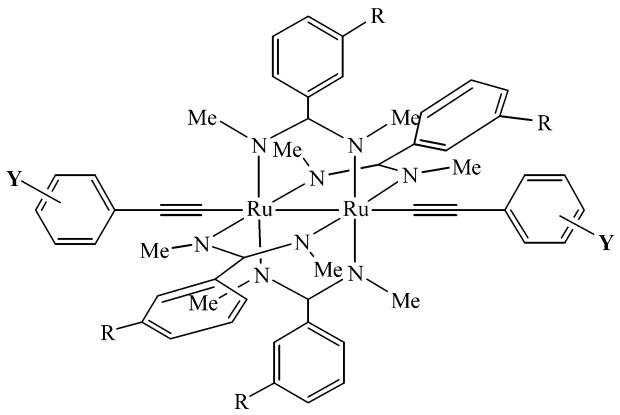

Y = *p*-H (**1a**/**b**), *p*-NO_2 (**2a**/**b**), *p*-CN (**3a**/**b**), *m*-CN (**4a**/**b**), *p*-NMe_2 (**5a**/**b**)
R = H (**a**) and *m*-MeO (**b**)

ease of alkynyl adduct formation at the $Ru_2(DMBA)_4$ core prompts us to consider its utility as the platform for the exploration of substituent electronic effects. Reported herein are the synthesis and characterization of the bis-adducts of substituted phenylethynyl ($YC_6H_4C{\equiv}C-$) on both $Ru_2(DMBA)_4$ and its derivative $Ru_2(m\text{MeO}DMBA)_4$ cores with their numerical designations defined in Chart 1.

Results and Discussion

Synthesis and Characterization of *σ*-Alkynyl Complexes. Synthesis of compound **1a** via the reaction between $Ru_2(DMBA)_4Cl_2$ and LiC_2Ph was reported previously.[24] However, the utility of lithiated alkynyl became less effective with phenylethynes bearing functional groups such as $-NO_2$ and $-CN$. For example, $Pt_2(\mu\text{-dppm})_2(C{\equiv}CC_6H_4\text{-}4\text{-}NO_2)_4$ was prepared from Pt(*P*,*P*′-dppm)Cl_2 and $LiC{\equiv}CC_6H_4\text{-}4\text{-}NO_2$ in only 21% yield.[25] We found that the newly reported complexes $Ru_2(DMBA)_4(NO_3)_2$ and $Ru_2(DMBA)_4(BF_4)_2$ readily reacted with *unactivated* alkynes in the presence of Et_3N at room temperature to yield the desired alkynyl derivatives:[26]

$$Ru_2(DMBA)_4(NO_3)_2 + 2HC_2R \xrightarrow[-(Et_3NH)NO_3]{Et_3N,\ THF,\ room\ temp} Ru_2(DMBA)_4(C_2R)_2$$

Under these conditions, compounds **1**−**4** formed in quantitative yields (monitored by thin-layer-chromatography), and workups were fairly straightforward. However, compounds **5a**,**b** could not be obtained similarly. Instead, they were prepared using the appropriate lithiated alkynyl. Alkynylation of a mononuclear Ru complex by 1-alkyne under weakly basic conditions is a well-established reaction, and the mechanism may involve the formation of a Ru−(η^2-HC≡CR) intermediate and its subsequent conversion to a Ru−vinylidene moiety.[27] This mechanism may not be operative in the current case, since the presence of four *N*-methyl groups will likely block the formation of a η^2-HC≡CR adduct on the Ru_2 core. Instead, the reaction may proceed via simple anion metathesis.

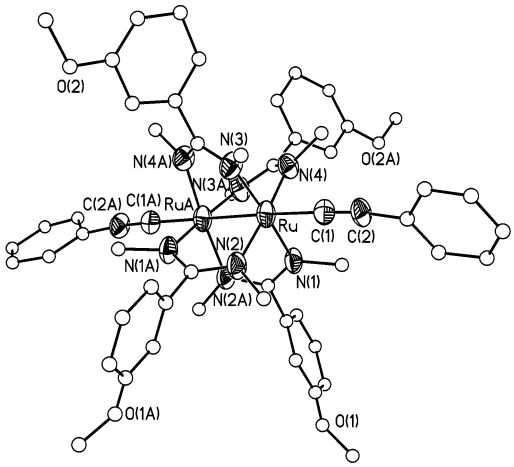

Figure 1. ORTEP plot of **1b** with ellipsoids at the 30% probability level.

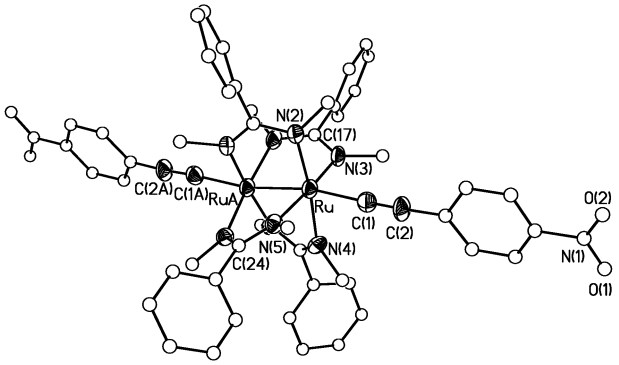

Figure 2. ORTEP plot of **2a** with ellipsoids at the 30% probability level.

The new compounds (**1b** and **2**−**5**) were characterized by combustion analysis, FAB mass spectrometry, ^{1}H NMR, visible−near-infrared (vis−near-IR), and IR spectroscopic techniques. The IR spectra generally display characteristic ν(C≡C) bands around 2070 cm^{-1}, accompanied by a ν(C≡N) band between 2217 and 2226 cm^{-1} in compounds **3** and **4**. The vis−near-IR spectra feature two intense absorption bands around ca. 515 and 883 nm, which are similar to the spectra reported for the series of $Ru_2(DMBA)_4(C{\equiv}CR)_2$ compounds with R = $SiMe_3$, C_2SiMe_3.[24] All the compounds reported herein are diamagnetic, with well-resolved ^{1}H NMR spectra, and the protons of the arylethynyl ligands can be unambiguously assigned in most cases.

Molecular structures of both compounds **1b** and **2a** determined via X-ray diffraction studies are shown in Figures 1 and 2, respectively, and the selected bond lengths and angles are collected in Table 1. Both molecules adopt the paddlewheel motif, and their general features are very similar to those reported earlier for $Ru_2(DMBA)_4(C_2R)_2$ with R = $SiMe_3$, C_2H.[24] The coordination spheres of the Ru centers can be described as pseudo-octahedral with four N centers from *DMBA* occupying the equatorial positions and the other Ru center and the alkynyl assuming two axial positions. The Ru−Ru bond length in **1b** (2.448(1) Å) is clearly

(25) Yam, V. W. W.; Hui, C. K.; Wong, K. M. C.; Zhu, N. Y.; Cheung, K. K. *Organometallics* **2002**, *21*, 4326.
(26) Xu, G.-L.; Jablonski, C. G.; Ren, T. *Inorg. Chim. Acta* **2003**, *343*, 387.
(27) Bruce, M. I. *Chem. Rev.* **1991**, *91*, 197.

Table 1. Selected Bond Lengths (Å) and Angles (deg) for Molecules 1b and 2a

1b		2a	
Ru−Ru′	2.4478(9)	Ru−Ru′	2.459(1)
Ru−N(1)	2.058(5)	Ru−N(2)	1.980(5)
Ru−N(2)	2.036(5)	Ru−N(3)	2.028(5)
Ru−N(3)	2.023(5)	Ru−N(4)	2.137(5)
Ru−N(4)	2.052(5)	Ru−N(5)	2.015(5)
Ru−C(1)	1.996(7)	Ru−C(1)	1.982(7)
C(1)−C(2)	1.20(1)	C(1)−C(2)	1.190(9)
N(1)−Ru−Ru	84.6(1)	N(2)−Ru−Ru′	94.7(2)
N(2)−Ru−Ru	88.6(1)	N(3)−Ru−Ru′	86.8(1)
N(3)−Ru−Ru	88.8(1)	N(4)−Ru−Ru	78.5(1)
N(4)−Ru−Ru	84.9(1)	N(5)−Ru−Ru′	86.5(1)
C(1)−Ru−Ru′	175.1(2)	C(1)−Ru−Ru′	165.5(2)
C(2)−C(1)−Ru	177.5(6)	C(2)−C(1)−Ru	176.3(7)

Table 2. Electrode Potentials and Related Data Determined using CV for Compounds 1−5

compd	σ_Y[a]	$E_{1/2}$(A)/V, ΔE/V, i_b/i_f[b]	$E_{1/2}$(B)/V, ΔE/V, i_b/i_f[b]
1a[c]	0	0.52, 0.058, 0.89	−1.10, 0.057, 0.79
1b	0	0.51, 0.058, 0.93	−1.10, 0.062, 0.80
2a	0.81	0.69, 0.069, 0.99	−0.87, 0.073, 0.92
2b	0.81	0.70, 0.067, 0.93	−0.86, 0.074, 0.68
3a	0.70	0.65, 0.065, 0.89	−0.92, 0.060, 0.93
3b	0.70	0.66, 0.065, 0.87	−0.94, 0.062, 0.98
4a	0.62	0.62, 0.063, 0.89	−0.98, 0.064, 0.93
4b	0.62	0.63, 0.066, 0.91	−0.98, 0.068, 0.99
5a	−0.83	0.31, 0.066, 0.95	−1.17[d]
5b	−0.83	0.29, 0.069, 0.88	−1.21[d]

[a] Taken from ref 32. [b] $i_b/i_f = i_{backward}/i_{forward}$. [c] Taken from ref 24. [d] E_{pc}, irreversible process.

shorter than that in **2a** (2.459(1) Å), while the Ru−C distance in **1b** is slightly longer than that in **2a**. As discussed previously,[9] the lengthening of the Ru−Ru bond in bis-alkynyl adducts is generally attributed to the formation of a strong σ(Ru−C) bond, which polarizes the d_{z^2} orbital toward the C center. The strong acceptor nature of 4-NO_2 groups in **2a** further enhances this effect. The ligand arrangement around the Ru_2 core in **2a** deviates significantly from the idealized D_4 symmetry, an effect commonly observed for *trans*-$Ru_2(L)_4(C_2Y)_2$ complexes and attributed to second-order Jahn−Teller distortion.[14] Interestingly, the deviation is negligible in **1b**.

Electrochemical Studies. The results of cyclic voltammetric (CV) measurements of the ruthenium alkynyl compounds **1**−**5** are summarized in Table 2. Previous work with diruthenium metallaynes revealed rich redox characteristics,[9] and the compounds described here are no exception. Compounds **1**−**5** generally feature two one-electron Ru_2-based couples: an oxidation (A), and a reduction (B), as shown by both the CVs of compounds ***n*a** (n = 2−5) in Figure 3 and those of ***n*b** provided in the Supporting Information. Both the oxidation and reduction couples are (quasi)reversible in compounds **1**−**4**, as evidenced by both small ΔE values and a near-unity $i_{backward}/i_{forward}$ ratio. The reduction couples in compounds **5a**,**b** are irreversible, and the irreversibility is indicative of alkynyl dissociation upon reduction.[24] Compounds **2a**,**b** also feature a second reduction around −1.29 V (C in the CV of **2a**), which is attributed to the reduction of the 4-NO_2 group on the basis of comparison with previous work.[28−30] Compounds **5a**,**b**, on the other hand, feature two additional oxidations at ca. 0.70 and

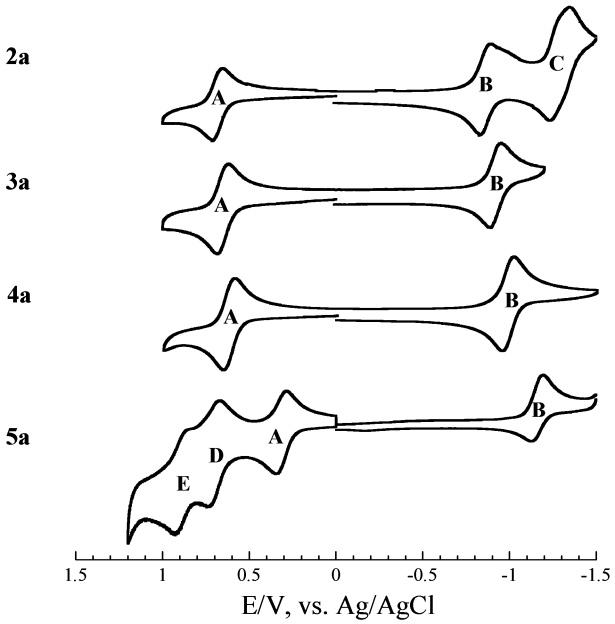

Figure 3. Cyclic voltammograms of complexes ***n*a** (n = 2−5) recorded in a 0.20 M THF solution of Bu_4NPF_6 at a scan rate of 100 mV/s.

0.90 V, respectively, which are clearly due to the sequential oxidations of two 4-NMe_2 groups.[31]

It is clear from Figure 3 that the electrode potentials for both the oxidation (A) and reduction couples (B) shift cathodically as the electron-withdrawing power of phenylethyne substituents decreases (NO_2 > CN > H > NMe_2). This trend can be further quantified by fitting the plot of electrode potentials versus the Hammett constant of substituent Y (σ_Y) according to the following equation:[32] $E_{1/2}(Y) = E_{1/2}(H) + \rho(2\sigma_Y)$, where ρ is the reactivity constant. Both the plot and fit for compounds ***n*a** (n = 1−5) are shown in Figure 4, and the reactivity constants are 110 and 86 mV for the oxidation (ρ(A)) and reduction (ρ(B)) processes, respectively. While the linear fit of oxidation potentials yields an excellent correlation coefficient (R = 99.5%), the linear fit of reduction potentials is of marginal quality (R = 95%), which is mainly due to the irreversibility of the reduction couple of compound **5a**. Similar reactivity constants (ρ(A) = 121 mV and ρ(B) = 97 mV) were obtained for compounds ***n*b** (n = 1−5), and the least-squares plots are provided in the Supporting Information (Figure S2). Comparison of both the ρ and electrode potentials in Table 2 between ***n*a** and ***n*b** series reveals that the redox processes associated with the Ru_2 core are relatively insensitive to the presence of substituents on the phenyl ring of *DMBA* ligands. Such a substituent independence, although surprising, can be explained by the fact that the phenyl group of the *DMBA* ligand is always far from being coplanar with the amidine group, due to the

(28) Hurst, S. K.; Cifuentes, M. P.; Morrall, J. P. L.; Lucas, N. T.; Whittall, I. R.; Humphrey, M. G.; Asselberghs, I.; Persoons, A.; Samoc, M.; Luther-Davies, B.; Willis, A. C. *Organometallics* **2001**, *20*, 4664.
(29) Yam, V. W. W.; Fung, W. K. M.; Cheung, K. K. *Organometallics* **1998**, *17*, 3293.
(30) Wu, I. Y.; Lin, J. T.; Luo, J.; Li, C. S.; Tsai, C.; Wen, Y. S.; Hsu, C. C.; Yeh, F. F.; Liou, S. *Organometallics* **1998**, *17*, 2188.
(31) Denis, R.; Toupet, L.; Paul, F.; Lapinte, C. *Organometallics* **2000**, *19*, 4240.
(32) Hansch, C.; Leo, A.; Taft, R. W. *Chem. Rev.* **1991**, *91*, 165.

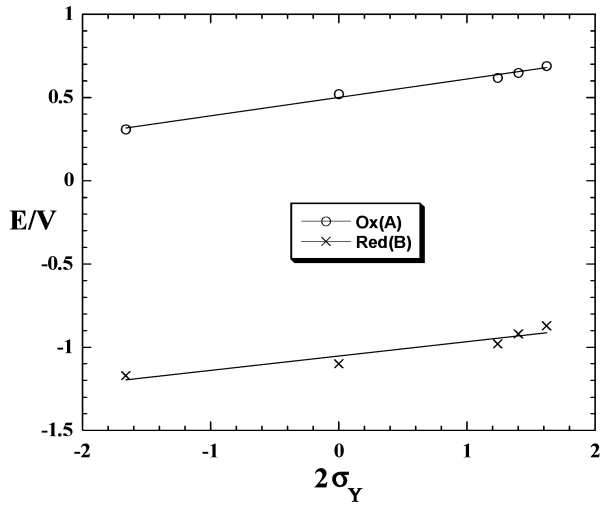

Figure 4. Hammett plot of $E_{1/2}$ vs 2σ. The crosses (×) are the measured values of $E_{1/2}$(B), circles (○) are the measured values of $E_{1/2}$(A), and the solid lines are the least-squares fit.

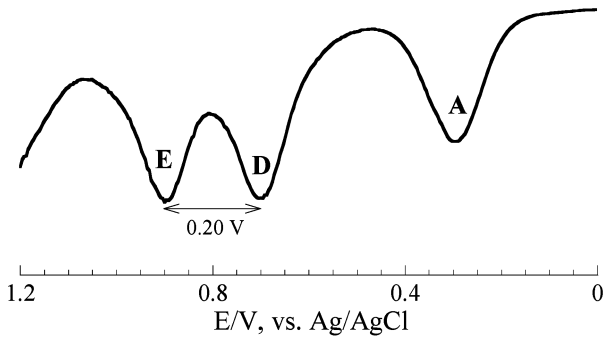

Figure 5. Differential pulse voltammogram of compound **5a** in the anodic region recorded in a 0.20 M THF solution of Bu_4NPF_6 at a scan rate of 4 mV/s.

presence of *N*-methyl groups, which effectively eliminates the propagation of electronic effect through conjugation.

The reactivity constants obtained for compounds **1**−**5** are comparable to the largest obtained for the M_2-(*D*Ar*F*)$_4$ series,[20] which is truly remarkable, considering that the substituted phenyl is only two bonds away from the M_2 center in the latter but three bonds away from the Ru_2 center in compounds **1**−**5**. The enhanced response to the substituent in compounds **1**−**5** indicates that the π-conjugation along the Ph−C≡C−Ru_2 backbone is extensive. Lapinte et al. reported the study of a comprehensive series of Cp*Fe(dppe)($C_2C_6H_4$-4-Y) compounds with Y = NO_2, CN, CF_3, F, Br, H, Me, ^{t}Bu, OMe, NH_2, NMe_2.[31,33,34] While a large range in $E°(Fe^{3+}/Fe^{2+})$ was observed, the electrode potentials do not correlate with σ_Y at all, and the lack of correlation was attributed to the coexistence of several canonical structures.

The stepwise appearance of 4-NMe_2 oxidation waves (D and E) in **5a** indicates that the mixed-valence species generated by the second oxidation (D) is delocalized. Although the separation between **D** and **E** could not be determined from the CV, it is readily determined from the differential pulse voltammogram of **5a** (Figure 5) as 0.20 V. Considering the fact that two NMe_2 groups are separated by over 20.0 Å (estimated from the structural data of **2a**), such a coupling strength is remarkable. In comparison, a ΔE value of 60 mV was reported for a bis(triarylamine) bridged by an organic linker over a distance of 19.3 Å.[35] The large ΔE value determined for **5a** reveals the exceptional ability of the Ru_2 metallayne in mediating electron delocalization. Unfortunately, the instabilities of the oxidized species preclude probing the intervalence charge-transfer transition to provide more insight into the electron delocalization in the mixed-valence species.

Conclusions

Alkynylation under weak base conditions adds a new dimension to the research of dinuclear alkynyl compounds and can be a powerful method to introduce other functionalized alkynes. Both the linear $E_{1/2}-\sigma_Y$ correlation and large reactivity constants for the Ru_2-based processes revealed the feasibility of achieving significant modulation of electronic structures of metallaynes through the substitution on axial phenylethynyls. We are currently investigating the synthesis of polar *D*C_6H_4C≡C−Ru_2−C≡CC_6H_4*A* type compounds (*D* and *A* are donor and acceptor substituents, respectively), which are similar to the molecular diode proposed by Ratner and Aviram.[36]

Experimental Section

General Conditions, Reagents, and Instruments. *n*-BuLi was purchased from Aldrich, PhC≡CH from Acros, and silica gel from Merck. $Ru_2(DMBA)_4Cl_2$,[24] Ru_2(*m*-MeO*DMBA*)$_4$-Cl_2,[37] $Ru_2(DMBA)_4(NO_3)_2$ and Ru_2(*m*-MeO*DMBA*)$_4(NO_3)_2$,[26] and 4-NO_2-C_6H_4C≡CH and 3-/4-CN-C_6H_4C≡CH[38] were prepared as previously described. 4-$Me_2NC_6H_4I$ was prepared via the method of Fabbrini et al.[39] and converted to 4-$Me_2NC_6H_4$C≡CH by the standard method. THF and hexanes were distilled over Na/benzophenone under a N_2 atmosphere prior to use. Infrared spectra were recorded on a Perkin-Elmer 2000 FT-IR spectrometer using KBr disks. Absorption spectra were obtained with a Perkin-Elmer Lambda-900 UV−vis−near-IR spectrophotometer. ^{1}H NMR spectra were recorded on a Bruker AVANCE 300 NMR spectrometer with chemical shifts (δ) referenced to the residual $CHCl_3$. Cyclic and differential pulse voltammograms were recorded in 0.2 M [NBu_4]PF_6 solution (THF, N_2-degassed) on a CHI620A voltammetric analyzer with a glassy-carbon working electrode (diameter 2 mm), a Pt-wire auxiliary electrode, and a Ag/AgCl reference electrode. The concentration of diruthenium species was always 1.0 mM. The ferrocenium/ferrocene couple was observed at 0.595 V (vs Ag/AgCl) under these experimental conditions. Elemental analysis was performed by Atlantic Microlab, Norcross, Georgia.

[Ru_2(*m*-MeO*DMBA*)$_4$(C≡CPh)$_2$] (1b). Ru_2(*m*-MeO*DMBA*)$_4$-$(NO_3)_2$ (134 mg, 0.129 mmol) was suspended in 20 mL of THF, to which were added HC≡CPh (104 mg, 1.02 mmol) and NEt_3 (5 mL). After the mixture was stirred for 20 h under argon, the solvent was removed under reduced pressure. The residue

(33) Paul, F.; Mevellec, J.-Y.; Lapinte, C. *J. Chem. Soc., Dalton Trans.* **2002**, 1783.
(34) Paul, F.; Costuas, K.; Ledoux, I.; Deveau, S.; Zyss, J.; Halet, J.-F.; Lapinte, C. *Organometallics* **2002**, *21*, 5229.
(35) Lambert, C.; Nöll, G. *J. Am. Chem. Soc.* **1999**, *121*, 8434.
(36) Aviram, A.; Ratner, M. A. *Chem. Phys. Lett.* **1974**, *29*, 277.
(37) Xu, G.-L.; Jablonski, C. G.; Ren, T. *J. Organomet. Chem.*, in press.
(38) Takahashi, S.; Kuriyama, Y.; Sonogashira, K.; Hagihara, N. *Synthesis* **1980**, 627.
(39) Fabbrini, M.; Galli, C.; Gentili, P.; Macchitella, D.; Petride, H. *J. Chem. Soc., Perkin Trans. 2* **2001**, 1516.

was loaded onto a silica gel column deactivated by 10% Et_3N in hexanes and eluted with ethyl acetate−hexanes−Et_3N (30/70/5, v/v), giving pure **1b** as a deep red material. Yield: 103 mg (72% based on Ru). Data for **1b** are as follows. R_f 0.41 (ethyl acetate−hexanes−Et_3N, 20/70/10, v/v; the same combination is also used for the determination of other R_f's). Anal. Found (calcd) for $C_{56}H_{62}N_8O_4Ru_2$: C, 60.65 (60.42); H, 5.49 (5.61); N, 10.07 (9.98). MS-FAB (*m/e*, based on ^{101}Ru): 1114 [MH^+]. UV−vis (λ_{max}, nm (ϵ, M^{-1} cm^{-1})): 874 (1500), 500 (9500). IR (cm^{-1}): ν(C≡C), 2071 (w). Electrochemistry ($E_{1/2}$, V; ΔE_p, V; $i_{backward}/i_{forward}$): A, 0.51, 0.058, 0.93; B, −1.10, 0.062, 0.80. ^{1}H NMR ($CDCl_3$, δ): 7.80−6.40 (26H, Ph), 3.81 (12H, OMe), 3.25 (24H, NMe).

[Ru_2(*DMBA*)$_4$(C≡C-4-$C_6H_4NO_2$)$_2$] (2a). $Ru_2(DMBA)_4(NO_3)_2$ (81.3 mg, 0.089 mmol) was suspended in 20 mL of THF, to which were added HC≡C-4-$C_6H_4NO_2$ (52.5 mg, 0.357 mmol) and NEt_3 (5 mL). The solution changed from dark green to red immediately upon the addition of the alkyne. After the mixture was stirred overnight under argon, the solution was filtered through a plug of deactivated silica, which was rinsed with CH_2Cl_2. The solvent was removed under reduced pressure, and the resulting solid was triturated with hexanes to yield pure **2a** as a deep red material. Yield: 91 mg (94% based on Ru). Data for **2a** are as follows. R_f 0.65. Anal. Found (calcd) for $C_{52}H_{52}N_{10}O_4Ru_2{\cdot}C_6H_{14}{\cdot}0.5CH_2Cl_2$: C, 58.22 (57.98); H, 5.53 (5.57); N, 11.40 (11.56). MS-FAB (*m/e*, based on ^{101}Ru): 1084 [MH^+]. UV−vis (λ_{max}, nm (ϵ, M^{-1} cm^{-1})): 859 (1820), 528 (24 100). IR (cm^{-1}): ν(C≡C), 2060 (m). Electrochemistry ($E_{1/2}$, V; ΔE_p, V; $i_{backward}/i_{forward}$): A, 0.69, 0.069, 0.99; B, −0.83, 0.073, 0.92, C, −1.29, 0.116, 0.79. ^{1}H NMR ($CDCl_3$, δ): 8.03 (J_{HH} = 9 Hz, 4H, C_6H_4), 7.48−7.38 (12H, Ph), 7.12 (J_{HH} = 9 Hz, 4H, C_6H_4), 7.01−6.94 (8H, Ph), 3.24 (24H, NMe).

[Ru_2(*m*-MeO*DMBA*)$_4$(C≡C-4-$C_6H_4NO_2$)$_2$] (2b). The synthesis is similar to that of **2a**, with $Ru_2(DMBA)_4(NO_3)_2$ being replaced by Ru_2(MeO-*m*-DMBA)$_4(NO_3)_2$. Yield: 74%. Data for **2b** are as follows. R_f 0.30. Anal. Found (calcd) for $C_{56}H_{60}N_{10}O_8Ru_2$: C, 55.65 (55.90); H, 5.22 (5.03); N, 11.13 (11.64). MS-FAB (*m/e*, based on ^{101}Ru): 1204 [MH^+]. UV−vis (λ_{max}, nm (ϵ, M^{-1} cm^{-1})): 855 (2500), 523 (34 600). IR (cm^{-1}): ν(≡CH), 2062 (m). Electrochemistry ($E_{1/2}$, V; ΔE_p, V; $i_{backward}/i_{forward}$): A, 0.70, 0.067, 0.93; B, −0.86, 0.074, 0.68, C, −1.29, 0.124, 0.64. ^{1}H NMR ($CDCl_3$, δ): 8.03 (J_{HH} = 9 Hz, 4H, C_6H_4), 7.80−7.20 (4H, Ph), 7.12 (J_{HH} = 9 Hz, 4H, C_6H_4), 7.00−6.40 (12H, Ph), 3.81 (12H, OMe), 3.26 (24H, NMe).

[Ru_2(*DMBA*)$_4$(C≡C-4-C_6H_4CN)$_2$] (3a). The synthesis is similar to that of **2a**, with 4-NO_2-C_6H_4C≡CH being replaced by 4-CN-C_6H_4C≡CH. Yield: 83%. Data for **3a** are as follows. R_f 0.61. Anal. Found (calcd) for $C_{54}H_{52}N_{10}Ru_2$: C, 61.09 (61.18); H, 5.05 (5.36); N, 12.16 (12.41). MS-FAB (*m/e*, based on ^{101}Ru): 1044 [MH^+]. UV−vis (λ_{max}, nm (ϵ, M^{-1} cm^{-1})): 869 (2900), 504 (18 800). IR (cm^{-1}): ν(C≡C), 2070 (m). Electrochemistry ($E_{1/2}$, V; ΔE_p, V; $i_{backward}/i_{forward}$): A, 0.65, 0.065, 0.89; B, −0.92, 0.060, 0.93. ^{1}H NMR ($CDCl_3$, δ): 7.50−7.35 (16H, C_6H_4 + Ph), 7.10 (J_{HH} = 8 Hz, 4H, C_6H_4), 7.00−6.95 (8H, Ph), 3.25 (24H, NMe).

[Ru_2(*m*-MeO*DMBA*)$_4$(C≡C-4-C_6H_4CN)$_2$] (3b). The synthesis is similar to that of **2b**, with PhC≡CH being replaced by 4-CN-C_6H_4C≡CH. Yield: 54%. Data for **3b** are as follows. R_f 0.25. Anal. Found (calcd) for $C_{58}H_{60}N_{10}O_4Ru_2{\cdot}CH_2Cl_2$ (**3b**·CH_2Cl_2): C, 56.98 (56.73); H, 5.01 (4.97); N, 11.12 (11.22). MS-FAB (*m/e*, based on ^{101}Ru): 1162 [$(M - H)^+$]. UV−vis (λ_{max}, nm (ϵ, M^{-1} cm^{-1})): 860 (2600), 479 (17 700). IR (cm^{-1}): ν(C≡C), 2066 (w). Electrochemistry ($E_{1/2}$, V; ΔE_p, V; $i_{backward}/i_{forward}$): A, 0.66, 0.065, 0.87; B, −0.94, 0.062, 0.98. ^{1}H NMR ($CDCl_3$, δ): 7.41 (J_{HH} = 8 Hz, 4H, C_6H_4), 7.40−7.30 (4H, Ph), 7.05 (J_{HH} = 8 Hz, 4H, C_6H_4), 7.00−6.45 (12H, Ph), 3.81 (12H, OMe), 3.25 (24H, NMe).

[Ru_2(*DMBA*)$_4$(C≡C-3-C_6H_4CN)$_2$] (4a). The synthesis is similar to that of **2a** with 4-NO_2-C_6H_4C≡CH being replaced by 3-CN-C_6H_4C≡CH. Yield: 64%. Data for **4a** are as follows. R_f 0.63. Anal. Found (calcd) for $C_{52}H_{52}N_{10}Ru_2$: C, 61.53 (62.17); H, 5.01 (5.02); N, 12.98 (13.43). MS-FAB (*m/e*, based on ^{101}Ru): 1046 [$(MH)^+$]. UV−vis (λ_{max}, nm (ϵ, M^{-1} cm^{-1})): 860 (2600), 502 (13 700). IR (cm^{-1}): ν(C≡C), 2073 (m); ν(C≡N), 2226 (w). Electrochemistry ($E_{1/2}$, V; ΔE_p, V; $i_{backward}/i_{forward}$): A, 0.63, 0.063, 0.89; B, −0.98, 0.064, 0.93. ^{1}H NMR ($CDCl_3$): 7.80−6.90 (28H, C_6H_4 + Ph), 3.25 (24H, NMe).

[Ru_2(*m*-MeODMBA)$_4$(C≡C-3-C_6H_4CN)$_2$] (4b). The synthesis is similar to that of **1b**, with PhC≡CH being replaced by 3-CN-C_6H_4C≡CH. Yield: 64%. Data for **4b** are as follows. R_f 0.26. Anal. Found (calcd) for $C_{58}H_{60}N_{10}O_4Ru_2{\cdot}CH_2Cl_2$ (**4b**·CH_2Cl_2): C, 56.68 (56.73); H, 5.03 (4.97); N, 11.03 (11.22). MS-FAB (*m/e*, based on ^{101}Ru): 1165 [$(MH)^+$]. UV−vis (λ_{max}, nm (ϵ, M^{-1} cm^{-1})): 857 (2600), 500 (14 100). IR (cm^{-1}): ν(C≡C), 2071 (m); ν(C≡N), 2226 (w). Electrochemistry ($E_{1/2}$, V; ΔE_p, V; $i_{backward}/i_{forward}$): A, 0.63, 0.066, 0.91; B, −0.98, 0.068, 0.99. ^{1}H NMR ($CDCl_3$, δ): 7.40−6.45 (4H, C_6H_4 + Ph), 3.80 (12H, OMe), 3.26 (24H, NMe).

[Ru_2(*DMBA*)$_4$(C≡C-4-$C_6H_4NMe_2$)$_2$] (5a). $Ru_2(DMBA)_4Cl_2$ (101 mg, 0.117 mmol) was dissolved in 20 mL of THF, to which was added LiC≡C-4-$C_6H_4NMe_2$ (0.45 mmol) prepared in situ from HC≡C-4-$C_6H_4NMe_2$ and *n*-BuLi. The solution changed from brown to dark red immediately upon the addition of the lithiated alkyne. After the mixture was stirred overnight under argon, the solvent was removed under reduced pressure. The residue was placed on a sintered funnel and washed with cold hexanes to give pure **5a** as a purple material. Yield: 40 mg (32%). Data for **5a** are as follows. R_f 0.66. Anal. Found (calcd) for $C_{56}H_{64}N_{10}Ru_2{\cdot}2CH_2Cl_2{\cdot}H_2O$ (**5a**·$2CH_2Cl_2{\cdot}H_2O$): C, 54.55 (54.93); H, 5.25 (5.52); N, 10.87 (11.05). MS-FAB (*m/e*, based on ^{101}Ru): 1080 [MH^+]. UV−vis (λ_{max}, nm (ϵ, M^{-1} cm^{-1})): 890 (2100), 511 (12 700). IR (cm^{-1}): ν(C≡C), 2078 (m). Electrochemistry ($E_{1/2}$, V; ΔE_p, V; $i_{backward}/i_{forward}$): A, 0.31, 0.066, 0.95; B, −1.17, 0.070, 0.41. ^{1}H NMR ($CDCl_3$, δ): 7.45−7.33 (12H, Ph), 7.00−6.95 (12H, C_6H_4 + Ph), 6.59 (J_{HH} = 9 Hz, 4H, C_6H_4), 3.28 (24H, N*Me*), 2.88 (12H, NMe_2).

[Ru_2(*m*-MeO*DMBA*)$_4$(C≡C-4-$C_6H_4NMe_2$)$_2$] (5b). Ru_2(*m*-MeO*DMBA*)$_4Cl_2$ (208 mg, 0.212 mmol) was dissolved in 25 mL of THF, to which was added LiC≡C-4-$C_6H_4NMe_2$ (0.854 mmol) prepared in situ from HC≡C-4-$C_6H_4NMe_2$ and *n*-BuLi. The solution changed from brown to dark red immediately upon the addition of the lithiated alkyne. After the mixture was stirred for 1 h under argon, the solvent was removed under reduced pressure. The residue was loaded onto a silica gel column deactivated by 10% Et_3N in hexanes and eluted with ethyl acetate−hexanes−Et_3N (30/70/5, v/v), giving pure **5b** as a deep red material. Yield: 86 mg (34%). The reduced yield is due to slow decomposition of **5b** on silica. Data for **5b** are as follows. R_f 0.15. Anal. Found (calcd) for $C_{66.5}H_{87}N_{10}O_4ClRu_2$ (**5b**·$C_6H_{14}{\cdot}^1/_2CH_2Cl_2$): C, 61.07 (60.14); H, 6.74 (6.60); N, 10.07 (10.55). MS-FAB (*m/e*, based on ^{101}Ru): 1200 [MH^+]. UV−vis (λ_{max}, nm (ϵ, M^{-1} cm^{-1})): 851 (1800), 504 (9800). IR (cm^{-1}): ν(C≡C), 2075 (w). Electrochemistry ($E_{1/2}$, V; ΔE_p, V; $i_{backward}/i_{forward}$): A, 0.29, 0.069, 0.88; B, −1.21, 0.00, 0.41. ^{1}H NMR ($CDCl_3$, δ): 7.41 (J_{HH} = 8 Hz, 4H, C_6H_4), 7.40−7.30 (4H, Ph), 7.05 (J_{HH} = 8 Hz, 4H, C_6H_4), 7.00−6.40 (12H, Ph), 3.79 (12H, OMe), 3.28 (24H, N*Me*), 2.86 (12H, NMe_2).

X-ray Data Collection, Processing, and Structure Analysis and Refinement. Single crystals of both compounds **1b** and **2a** were grown via slow evaporation of the fractions from column purification. The X-ray intensity data were measured at 300 K on a Bruker SMART1000 CCD-based X-ray diffractometer system using Mo Kα radiation (λ = 0.710 73 Å). Crystals of dimension 0.58 × 0.46 × 0.23 mm^3 (**1b**) and 0.39 × 0.13 × 0.06 mm^3 (**2a**) were cemented onto a quartz fiber with epoxy glue for X-ray crystallographic analysis. Data were measured using ω scans of 0.3° per frame such that a hemisphere (1271 frames) was collected. No decay was indicated for either data set by the re-collection of the first 50 frames at the end of each data collection. The frames were integrated with the Bruker SAINT software package using a

narrow-frame integration algorithm,[40] which also corrects for the Lorentz and polarization effects. Absorption corrections were applied using SADABS, supplied by George Sheldrick.

The structures of both **1b** and **2a** were solved and refined using the Bruker SHELXTL (version 5.1) software package in the space group *C*2/*c*.[41−43] Positions of all non-hydrogen atoms of diruthenium moieties were revealed by direct methods. In each case, the asymmetric unit contains half of the diruthenium molecule, which is related to the other half via a crystallographic 2-fold axis orthogonal to and bisecting the Ru−Ru′ vector. One of the phenyl rings of the *DMBA* ligand in **1b** was severely disordered and consequently refined as a rigid hexagon. With all non-hydrogen atoms being anisotropic and all hydrogen atoms in calculated position and riding mode, both structures were refined to convergence by least-squares methods on F^2, SHELXL-93, incorporated in SHELXTL.PC version 5.03. Relevant information on the data collection and the figures of merit of final refinement are listed in Table 3.

Table 3. Crystal Data for Compounds 1b and 2a

	1b	**2a**·$2CH_2Cl_2$
formula	$C_{56}H_{62}N_8O_4Ru_2$	$C_{54}H_{56}Cl_4N_{10}O_4Ru_2$
fw	1113.3	1253.0
space group	*C*2/*c*	*C*2/*c*
a, Å	19.845(2)	21.366(3)
b, Å	15.222(2)	18.020(3)
c, Å	19.967(2)	16.741(3)
β, deg	116.806(3)	115.581(2)
V, Å^3	5383.6(9)	5814(2)
Z	4	4
ρ_{calcd}, g cm^{-3}	1.374	1.432
μ, mm^{-1}	0.613	0.755
T, °C	27	27
no. of rflns collected	13 691	21 507
no. of indep rflns	4740 (*R*(int) = 0.0763)	5107 (*R*(int) = 0.1162)
final *R* indices ($I > 2\sigma(I)$)	R1 = 0.065, wR2 = 0.186	R1 = 0.064, wR2 = 0.1372

Acknowledgment. We thank both the University of Miami and the National Science Foundation (Grant No. CHE 0242623) for financial support. G.-L.X. thanks the University of Miami for a Maytag Graduate Fellowship.

Supporting Information Available: Tables of X-ray crystallographic data and figures giving additional ORTEP views for the structure determination of compounds **1b** and **2a**; X-ray data are also available as electronic CIF files. This material is available free of charge via the Internet at http://pubs.acs.org.

OM030401Y

(40) SAINT V 6.035 Software for the CCD Detector System; Bruker-AXS Inc., 1999.

(41) SHELXTL 5.03 (Windows NT Version), Program Library for Structure Solution and Molecular Graphics; Bruker-AXS Inc., 1998.

(42) Sheldrick, G. M. SHELXS-90, Program for the Solution of Crystal Structures; University of Göttingen, Göttingen, Germany, 1990.

(43) Sheldrick, G. M. SHELXL-93, Program for the Refinement of Crystal Structures; University of Göttingen, Göttingen, Germany, 1993.